Large Format Geiger-mode Avalanche Photodiode LADAR Camera

Ping Yuan*, Rengarajan Sudharsanan, Xiaogang Bai, and Eduardo Labios
Spectrolab Inc., a Boeing Company, 12500 Gladstone Ave., Sylmar, CA, USA 91342

Bryan Morris, John P Nicholson, Gary M Stuart, and Harrison Danny
Boeing DES, 4411 The 25 Way NE # 350, Albuquerque, NM 87109

ABSTRACT

Recently Spectrolab has successfully demonstrated a compact 32x32 Laser Detection and Range (LADAR) camera with single photo-level sensitivity with small size, weight, and power (SWAP) budget for three-dimensional (3D) topographic imaging at 1064 nm on various platforms. With 20-kHz frame rate and 500-ps timing uncertainty, this LADAR system provides coverage down to inch-level fidelity and allows for effective wide-area terrain mapping. At a 10 mph forward speed and 1000 feet above ground level (AGL), it covers 0.5 square-mile per hour with a resolution of 25 in^2/pixel after data averaging. In order to increase the forward speed to fit for more platforms and survey a large area more effectively, Spectrolab is developing 32x128 Geiger-mode LADAR camera with 43 frame rate. With the increase in both frame rate and array size, the data collection rate is improved by 10 times. With a programmable bin size from 0.3 ps to 0.5 ns and 14-bit timing dynamic range, LADAR developers will have more freedom in system integration for various applications. Most of the special features of Spectrolab 32x32 LADAR camera, such as non-uniform bias correction, variable range gate width, windowing for smaller arrays, and short pixel protection, are implemented in this camera.

1. INTRODUCTION AND BACKGROUND

SWIR 3D imaging provides one more important dimension in military and civilian imaging and aerial mapping applications. Because the laser and its service system takes most of a LADAR system SWAP, it is essential to maximize the camera sensitivity to reduce the laser power in order to enhance the ranging distance and reduce the SWAP of the whole system. By reaching the optical detection quantum limit, InP-based single-photon counting Geiger-mode avalanche photodiodes (GM-APD) fit perfectly to this requirement. SWIR GM-APD focal plane arrays (GM-FPAs) have been reported by both MIT Lincoln Laboratory[1] and Boeing Spectrolab[2]. In order to cover a large area quickly and efficiently with high resolution at high altitude, it is critical to develop large-format single-photon sensitive Geiger-mode LADAR cameras.

Large-format LADAR cameras imposes serious challenges to both APD array and ROIC designs. As the imaging array size grows, the pitch of the pixels has to be reduced in order to restrict the size and weight of the optical system. The optical crosstalk has to be carefully controlled as the distance between pixels is reduced, while they have to maintain low dark count rate (DCR) and high photon detection efficiency (PDE). Coupled with higher frame rate, which is preferred for operation with fiber lasers, a larger arrays size will generate a much larger amount data. From Spectrolab 32x32 20kHz LADAR camera to Spectrolab 32x128 43 kHz camera, the data throughput increased by about 7x to 2.8 Gb/s. So, data downloading and processing need to be carefully considered in both ROIC and camera designs for larger-format cameras. At the same time, because the higher pixel density and higher frame rate can greatly increase the ROIC thermal density, the power consumption of each ROIC pixel and heat dissipation in the camera have to be strictly controlled.

* Email: ping.yuan@boeing.com; Tel: 818 898 7578; Fax : 818 838 7474.

We have been improving the performance of both the avalanche photodiode detector and ROIC arrays that together comprise an FPA. The enhanced capabilities of the newly designed 32x32 ROIC include non-uniform bias (NUB) correction and shorted pixel protection. Instead of biasing the whole array with a single voltage in most focal plane arrays (FPA), NUB can tune the bias individually to pixels with 4-bit resolution and in a 2.5 V range. High voltage is applied to pixels to operate in Geiger mode. A single pixel shorting out of the thousands of pixels can reduce the array APD bias, overheat the local area, and cause an FPA failure. The short-related failure may occur in the array fabrication, FPA assembly, and later usage. In order to improve the FPA yield, uniformity, and reliability, the pixel input circuit was modified and effectively removed high dark current (shorted) APD pixels from the array to reduce the overall current draw of an APD array. Spectrolab has also introduced a feature to the APD detector array that reduces the optical crosstalk between pixels to <100ppm and reduces Dark Count Rate (DCR) at operating temperature to 3-4 kHz . External PDE on detectors alone, without a microlens, in excess of 40% has been demonstrated for reverse-illuminated arrays. With external clocks, the FPA demonstrated little pulse skew or chirp across the whole gate.

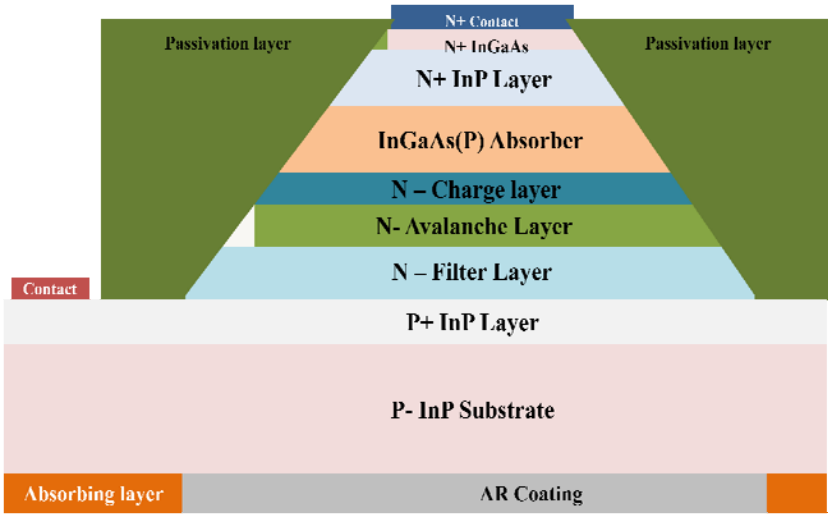

Figure 1 The mesa structure used for the Geiger-mode APD pixels. InGaAsP absorber is used for 1.06 um wavelength applications. For 1.55 um wavelength, it will be replace with InGaAs.

2. GM-APD DEVICE

In order to achieve higher pixel density and minimize the crosstalk and afterpulsing for large format arrays, we chose the mesa structure shown in Figure 1 for the Geiger-mode APD pixels. InGaAsP absorber is used for 1.06 um wavelength applications. For 1.55 um wavelength, it will be replaced with InGaAs. In order to suppress the optical crosstalk due to the secondary emission from the avalanche layer, a N-filter layer is implemented to selectively absorb it. The mesas are passivated and planarized after device formation.

In Geiger-mode operation the APDs are biased above the breakdown voltage for a short period of time. Due to various carrier generation mechanisms, they have some probability to generate output pulses even without any incident photons. This probability is dark count rate (DCR) and it represents the noise of GM-APDs. The maximum length of this Geiger-mode period is also determined by DCR. If there is an incident signal photon in this period, it has a probability to be absorbed and multiplied in the GM-APD such that the amplitude of the result pulse is large enough to be converted into a digital pulse that can be registered by the following readout circuit. This probability is another figure of merit of Geiger-mode APDs, photon detection efficiency (PDE).

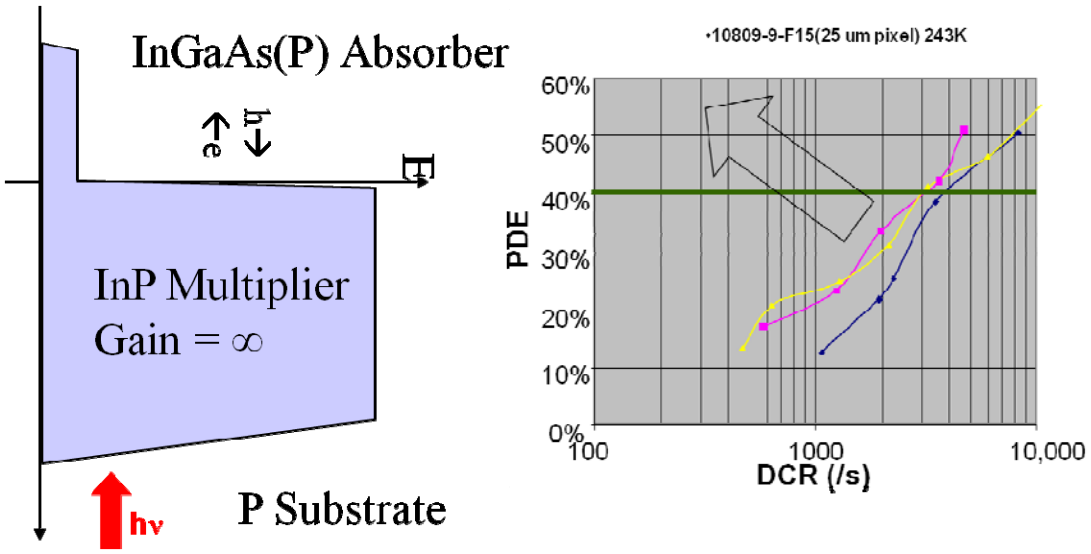

Figure 2 The electric field profile during operation Geiger-mode operation of an APD. The right panel shows PDE as function of DCR of three typical Spectrolab 25-µm diameter Geiger-mode APD pixels of a 32x128 array. The data are measured at various overbias points and at 243 K.

In order to minimize the dark current generation in the narrow band absorber and maximize gain in the multiplier, the InGaAsP/InP GM-APD separate absorption and gain and multiplication (SAGM) device structure is tuned for 1.06 µm operation and the electric field profile is shown in

Figure 2. Because both DCR and PDE increase with the overbias, for a better signal-to-noise ratio, the device operation point has to be carefully selected for the trade-off between PDE and DCR. The right panel plots the PDE against DCR of three 25-µm array pixels on a 32x128 GM APD array under different overbiases and at 243K. Grown on p-type InP substrates, the devices can achieve 40% PDE with 3~4 kHz DCR at the operation temperature. The device growth, process and characterization details have been reported previously[2,3].

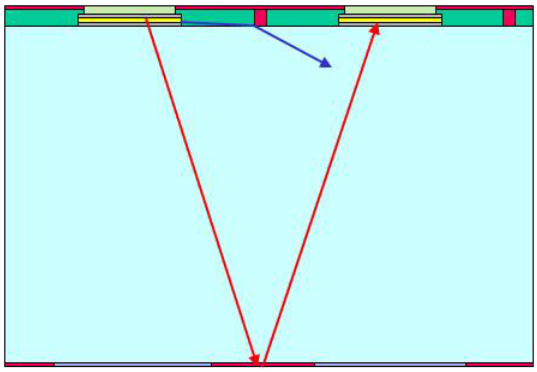

Figure 3 The two propagation paths for the secondary emission to a neighbor. The red line shows the surface emission reflected by the bottom. The blue line shows the lateral emission likely deflected to the high index substrate.

In each avalanche event, due to photon detection or dark count, a large amount of free carriers will be generated through the impact ionization process. The highest density of both carriers appears in the multiplication layer, and the probability of radiative recombination is non-negligible. Because all pixels in a GM APD array are biased beyond the breakdown voltage and they are extremely sensitive to single photon level in the detection gate, any secondary emission from a neighbor pixel can trigger false detections. If this crosstalk probability is not well controlled, the chain reaction can turn on the whole array with a single input photon and severely degrade the LADAR image quality. As the pixel pitch reduced from 100 μm of the previously reported 32x32 GM APD arrays to 50 μm, the crosstalk is an even greater concern.

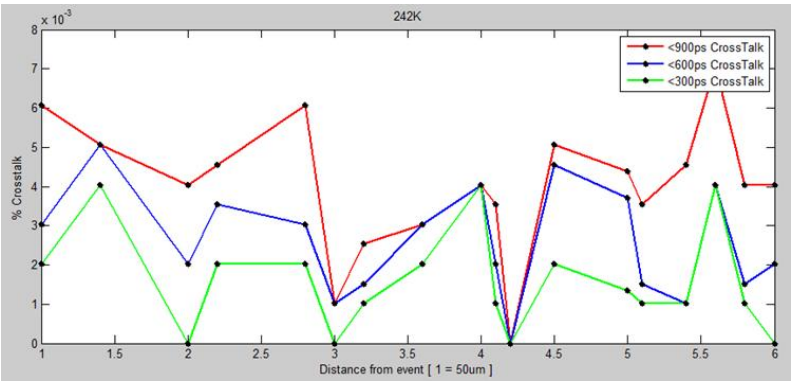

Figure 4 The crosstalk probability as a function of the distance to the initiating pixel of a 50 um-pitch 32x128 Geiger-mode APD array under 4-V overbias. The pixel to pixel crosstalk is less than 60 ppm.

In general, the secondary emission has two paths to propagate to the neighbors: surface emission and lateral emission. Due to the top metal contact, the surface emission can only go through the InP substrate. Because the secondary emission is primarily at the wavelength of the multiplier bandgap, the absorption in the N-filter layer in Figure 1 makes the first barrier for the crosstalk. The bottom of the array is covered by the AR coated incident window and metalized contact. The leftover secondary photons will either go through the AR coating with little reflection or get absorbed by another absorption layer deposited with the metal contact. For large pitch arrays, the solid angle of the cross section of the neighbor pixels is very small and the lateral emission is often of less concern. Compared to planar APD structures, the low index passivation layer gives mesa devices another layer of protection. Because of the high index contrast between the InP substrate and passivation material, the passivation layer between pixels makes a very lossy waveguide such that even less secondary photons can make the way to the neighbors. Figure 4 shows the pixel to pixel crosstalk of a 50 um-pitch 32x128 Geiger-mode APD array under 4-V overbias. The distance is in the unit of pixel pitch, and the crosstalk is less than 60 ppm, or 0.006% for all the distances.

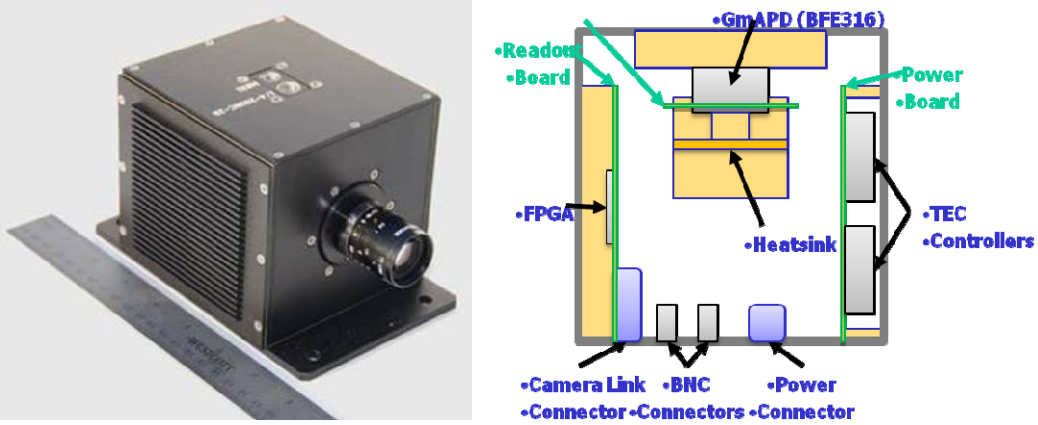

Figure 5 Spectrolab 32x32 Geiger-mode LADAR camera and its internal configuration.

Parameter	Unit	SPL SCA
Format		32x32
Pitch	um	100
Max frame rate	kHz	20
Bin size	ns	0.5
Jitter	ns	0.43
Output		Basic CL
Volume	In	4x4x4
Power	W	25

Table 1 The specifications of Spectrolab 32x32 Geiger-mode APD LADAR camera.

3. SPECTROLAB GEN-II 32X32 LADAR CAMERA

With capacities in MOVPE epitaxy, wafer process, and module packaging, Spectrolab vertically integrated the LADAR camera manufacturing in house. After the detector array fabrication, Indium bumps were evaporated on to the array pixels. The detector array was integrated with a ROIC of the same format by flip-chip bonding. A GaP microlens array was attached to the focal plane array for a better fill factor afterward. The FPA and the interposer were mounted on to a TE cooler and the assembly was soldered in a 69-pin grid array package. Later, the package was hermetically sealed with an AR-coated sapphire window. Under the support of DARPA, a 32x32 readout-integrated circuit (ROIC was designed in 180-nm CMOS technology. Many improvements were incorporated in this design based on our experience with the previous versions. They include: short pixel protection, 4-bit APD array NUB correction, 6.7 μs gate width with 0.5 ns resolution (or 1000 m range with 7.5 cm resolution), 435-ps whole system jitter, negligible chirp and pulse skew, and 300 mW power consumption. Figure 5 shows the picture of this camera and its internal configuration. Table 1 lists the basic specifications of the Spectrolab 32x32 Geiger-mode APD LADAR camera.

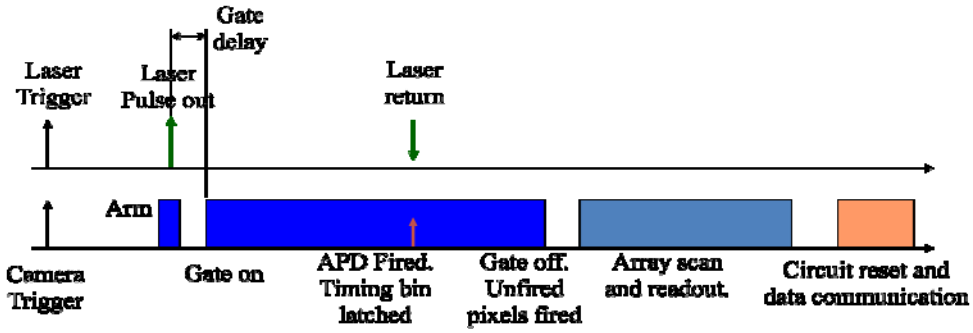

Figure 6 The timing and operation sequence of a detection cycle of Spectrolab 32x32 Geiger-mode APD LADAR camera.

Figure 6 illustrates the timing and operation sequence of a detection cycle of this LADAR camera. The trigger can be generated internally or externally. Before the delivery, the trigger format will be selected between LVDS or LVTTL. The synchronization with the laser is realized with the isolated BNC trigger input and output ports on the back of the camera. After the camera is triggered, the sensor array will be armed and ready for detection. The delay between the trigger and gate-on is a combination of the circuit internal delay, which is about 80-100 ns, and the user specified gate delay. If the camera is used as a trigger master, a laser delay relative to the camera trigger can also be inserted. As a result, there will be a delay between the laser pulse out and sensor gate on, which defines the nearest range of this configuration while the sensor gate width determines the sensitive range from this point. By changing this delay, the camera sensitive range can be shifted from 0 m to the maximum range allowed by the sensor sensitivity, the laser power, and optics. If there is optical return in the sensitive range or sensor gate, the imaging pixels will be fired and the timing bins of these pixels will be latched in registers till the end of the gate. So, the fired pixels will remain blind in the rest of the gate period. With a bin size of 0.5 ns, the Spectrolab camera has a ranging resolution of 7.5 cm without interpolation. The 14-bit timing dynamic range enables a usable gate up to 6.7 us, or 1 km. At the end of the gate, the unfired pixels are forced to fire such that all the registers have ranging information. Then, the ranging information is scanned and downloaded, and the circuit is reset.

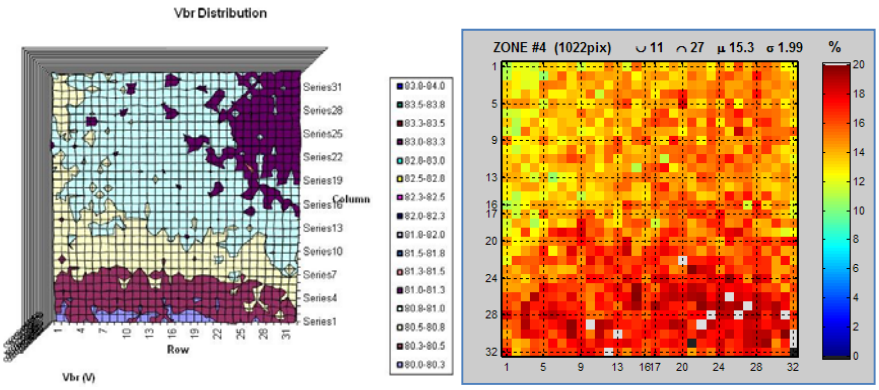

Figure 7 Uniformity of a 32x32 array. The left panel shows the breakdown voltage map of a 32x32 APD array. Each color represents a 0.25 V voltage range. The breakdown voltage increases from the lower left corner to the upper right corner. The right panel shows the firing probability map of the same array under a uniform bias and uniform illumination.

Uniformity is a critical array and camera performance. As shown in Figure 7, APD arrays have natural variations in breakdown voltage, which results in a performance variation across the array if it is biased under a uniform bias. As the breakdown voltage increases from the lower left corner to the upper right

corner, the sensitivity decreases in the same pattern in a camera assembled with this array under a uniform bias and uniform illumination.

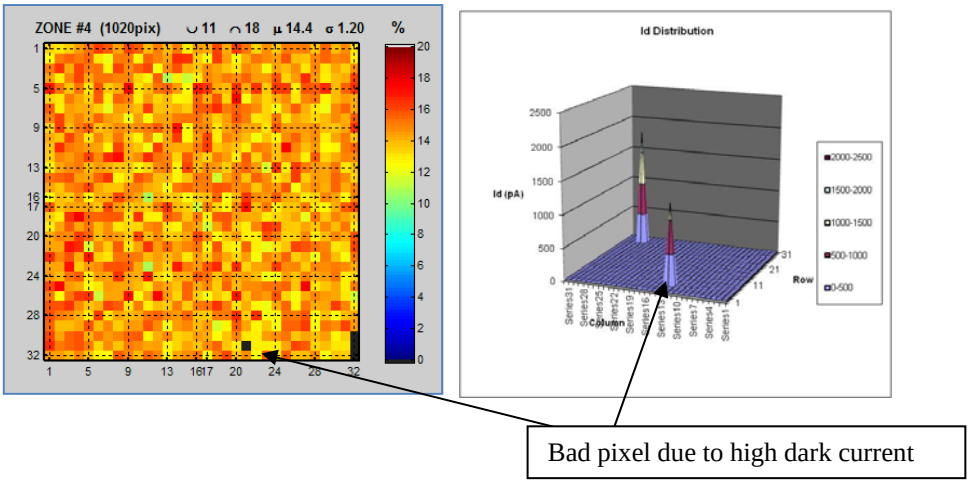

Figure 8 The firing probability map of the same 32x32 array after NUB correction and its array dark current map.

By introducing a 4-bit 2.5V in-pixel programmable NUB adjustment, the Spectrolab 32x32 LADAR camera can program the bias of each individual pixels and improve the array sensitivity uniformity. Figure 8 shows the firing probability map of the same 32x32 array after this NUB correction, and the standard deviation of the firing probability decreases from 1.99% to 1.20%. Obviously, the sensitivity uniformity of the camera is greatly improved.

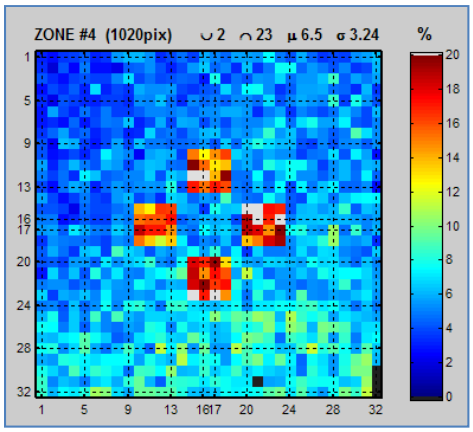

Figure 9 The Firing probability map of the same 32x32 array after NUB programming to enhance the sensitivity of four 4x4 regions.

This function also allows array windowing: increased or decreased sensitivity within a specified region. Figure 9 demonstrated four 4x4 regions with enhanced sensitivity near the array center. Working like a digital optical aperture, this windowing function can avoid the interference and cross talk from other pixels out of the target area.

Short pixel protection is another important feature implemented in this ROIC. With the immunity to sparse shorted detectors normally in APD arrays, this protection in the front end circuit greatly improves manufacturability and stability of FPAs.

The ROIC power consumption is reduced to 300 mW, about 50% of the previous version. Because the FPA is at the top of several stages of TECs, which consume most of the power in a LADAR camera, the nearly halved ROIC power consumption dramatically reduced the camera power load and heatsink weight.

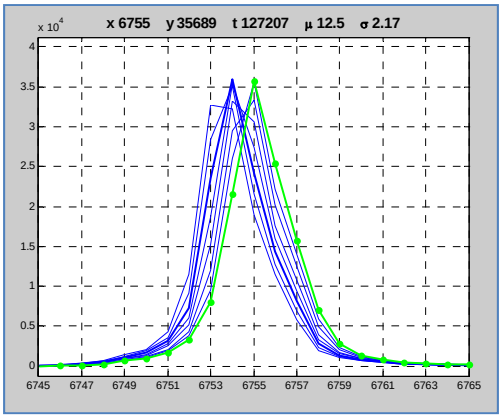

NEGATIVE SKEW @ 100psec

Run#	Dly:ns	Rng:bin	Δ:ps	std
ZERO	4000.0	6755.34	±001	879
Neg1	3999.9	6755.10	-117	903
Neg2	3999.8	6754.93	-202	906
Neg3	3999.7	6754.69	-323	883
Neg4	3999.6	6754.52	-411	882
NEG5	3999.5	6754.32	-509	885
Neg6	3999.4	6754.13	-605	881
Neg7	3999.3	6753.91	-715	906

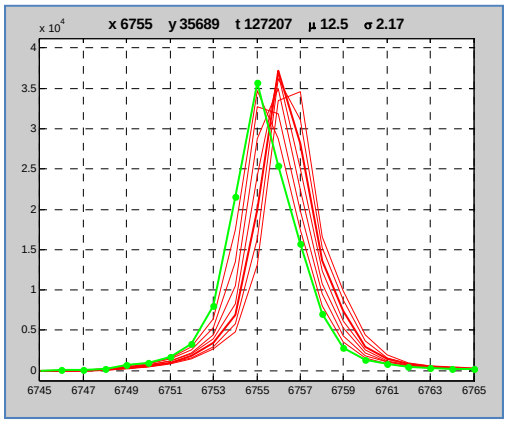

POSITIVE SKEW @ 100psec

Run#	Dly:ns	Rng:bin	Δ:ps	std
ZERO	4000.0	6755.34	±002	882
Pos1	4000.1	6650.43	+91	879
Pos2	4000.2	6650.48	+194	877
Pos3	4000.3	6650.70	+310	843
Pos4	4000.4	6651.02	+400	848
POS5	4000.5	6651.21	+510	873
Pos6	4000.6	6651.44	+599	872
Pos7	4000.7	6651.67	+687	874

Figure 10 Possitive and negative pulse skew of a 2ns laser pulse. 100 ps pulse resolution is demonstrated.

With data accumulated from multiple frames and/or large objects, the pulse amplitude information can be extracted from the timing histogram. By interpolating the pulse magnitude, the pulse timing resolution can be improved beyond the limit of the timing bin size. A 2 ns laser pulse was moved by 100 ps in delay each time as shown in Figure 10. In both directions, the camera can easily distinguish the delay difference in the histogram with a resolution no less than 100 ps, though the pulse width is 2 ns and the bin size is 500 ps.

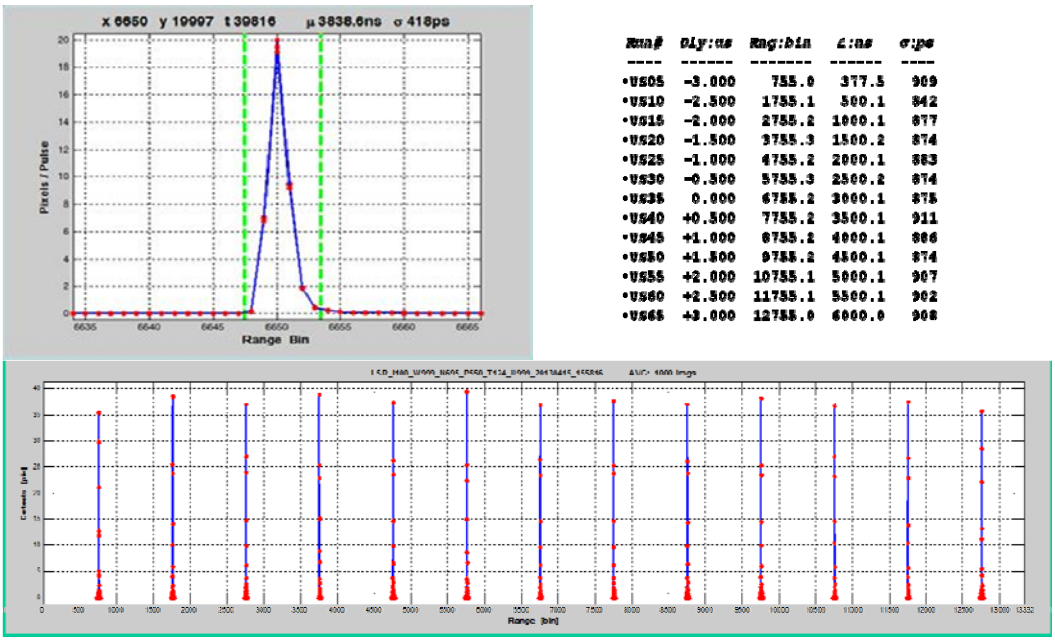

Figure 11 The top graph shows the temporal histogram of a single laser pulse detected by a Spectrolab 32x32 LADAR camera. The overall system RMS jitter is about 418 ps. The bottom panel shows a series of signals detected from laser pulses delayed by 500 ns from each other. The data of all the delays is attached.

The ranging accuary of a LADAR camera is determined by its overall jitter and chirp performance. The temporal histogram of our Gen-II 32x32 camera to a synchronized 90 ps laser pulse is shown in the top panel of Figure 11. The bin size is 500 ps, and the laser pulse width is included in this measurement. By calculating the standard deviation of this temporal distribution, we can get the overall system RMS jitter of 418 ps, which includes the laser pulse width and jitters in the trigger loop, APDs, ROIC, and readout boards and is shorter than the 500ps bin size. With a new clock design, the chirp in this camera is negligible. As shown in the bottom panel of Figure 11, by increasing the delay of a laser pulse 500 ns each time, we have got a series of evenly spaced signals in the detection gate. The error of the pulse spaces is controlled within 0.1 ps, which matches well with the ranging resolution demonstrate above.

4. SPECTROLAB 32X128 LADAR CAMERA

For higher aerial mapping and 3D imaging efficiency, Spectrolab developed a 32x128 GM-APD SCA as reported previously[3]. Based on this effort and the experience in our 32x32 SCAs, the commercial 32x128 SCA has incorporated many new features, including full Cameralink control and output, 50 kHz frame rate at all gate width, programmable 0.3 ~ 0.5 ns bins, 14-bit timing resolution, short pixel protection, and 4-bit NUB correction. Although the size is four times of that of the 32x32 SCAs, the power consumption is kept at 600 mW. Compared to Spectrolab 32x32 20kHz LADAR camera, the higher frame rate and larger format increase the data throughput by about 7x to 2.8 Gb/s. Full CameraLink and Coaxpress control and output ports will be implemented in this camera.

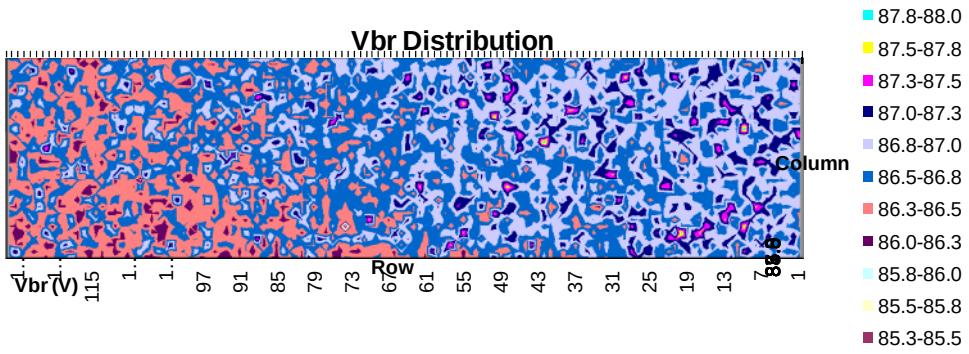

Figure 12. The breakdown voltage map of a 32x128 APD array at room temperature. Each color represents a 0.25 V range.

The 32x128 APD arrays were fabricated with improved dark current uniformity and crosstalk performance. The breakdown voltage map is shown in Figure 12, and its range is well within the NUB capacity.

The FPA is located in the center of the SCA. Similar to the 32x32 SCAs, the final assembly will be hermetically sealed in a 160-pin PGA package with the same size and footprint. Based on this SCA development, the next generation GmAPD 32x128 LADAR camera will be demonstrated soon.

5. SUMMARY

For large format SWIR LADAR cameras, Spectrolab developed the technologies for uniform small pitch array fabrication, small-pitch array crosstalk suppression, large data stream handling, and low power ROIC operation. With these technologies, Spectrolab demonstrated Geiger-mode APD arrays with 3-4 kHz DCR with 40% PDE, 60 ppm pixel-pixel crosstalk probability with 50 um pitch, and 0.16-V breakdown voltage standard deviation. Assembled with the arrays and newly developed ROIC, the Spectrolab 32x32 LADAR camera can open the gate up to 1 km with 0.5 ns bin size. The pulse skew tests show the measurement resolution can be improved to 100 ps with little chirp across the whole gate. The NUB function greatly improved the camera sensitivity uniformity. The 32x128 LADAR camera, currently under development, inherits all the features from the 32x32 version with large format and 43 kHz frame rate.

ACKNOWLEDGEMENTS

We would like to acknowledge the invaluable assistance provided by MIT Lincoln Laboratory and early stage funding from DARPA (Contract HR0011-08-C-0020) over the last several years.

REFERENCES

[1] K. A. McIntosh, et al., “Arrays of III-V semiconductor Geiger-mode avalanche photodiodes,” Lasers and Electro-Optics Society, 2003. LEOS 2003. The 16th Annual Meeting of the IEEE. Volume 2, 686 (2003).

[2] R. Sudharsanan, et al., “Single photon counting Geiger Mode InGaAs(P)/InP avalanche photodiode arrays for 3D imaging,” *Proc. SPIE* 6950, 69500N (2008).

[3] P. Yuan, et al., “Geiger-mode LADAR cameras,” *Proc. SPIE* 8037, 803712 (2011).